

Orthogonality of Zernike Polynomials

Victor Genberg, Gregory Michels
Sigmadyne, Inc. Rochester, NY

Keith Doyle
Optical Research Associates, Westborough, MA

ABSTRACT

Zernike polynomials are an orthogonal set over a unit circle and are often used to represent surface distortions from FEA analyses. There are several reasons why these coefficients may lose their orthogonality in an FEA analysis. The effects, their importance, and techniques for identifying and improving orthogonality are discussed. Alternative representations are presented.

Keywords: Opto-Mechanical Analysis, Zernike polynomials, Orthogonality

1.0 CONTINUOUS DATA

1.1 Orthogonal Functions

Two functions F_1 and F_2 are orthogonal over a unit circle if:

$$\int_0^1 \int_0^{2\pi} F_1 F_2 r d\Theta dr = 0 \quad (1.1)$$

For axisymmetric functions with no Θ variation, the above equation reduces to:

$$2\pi \int_0^1 F_1 F_2 r dr = 0 \quad (1.2)$$

Consider the axisymmetric functions:

$$\Psi_1 = r^2 \quad \Psi_2 = r^4 \quad (1.3)$$

which are the Seidel terms for Power and Primary Spherical. Integrating over the unit circle shows that these are not orthogonal:

$$2\pi \int_0^1 (r^2)(r^4)r dr = 2\pi \int_0^1 r^7 dr = 2\pi \left(\frac{1}{8} \right) \neq 0 \quad (1.4)$$

However if the functions are modified as follows,

$$\Phi_1 = 2r^2 - 1 \quad \Phi_2 = 6r^4 - 6r^2 + 1 \quad (1.5)$$

orthogonality is obtained

$$\begin{aligned} 2\pi \int_0^1 (2r^2 - 1)(6r^4 - 6r^2 + 1)r dr &= 2\pi \int_0^1 (12r^7 - 18r^5 + 8r^3 - r) dr = \\ 2\pi \left(\frac{12}{8} - \frac{18}{6} + \frac{8}{4} - \frac{1}{2} \right) &= 0 \end{aligned} \quad (1.6)$$

The functions Φ_1 and Φ_2 above are the Zernike polynomials for Power and Primary Spherical. Note that these functions are also orthogonal to Bias ($\Phi_0=1$). For example, the integral of Bias and Power is:

$$2\Pi \int_0^1 (1)(2r^2 - 1)rdr = 2\Pi \left(\frac{2}{4} - \frac{1}{2} \right) = 0 \quad (1.7)$$

Thus Zernike polynomials were orthogonalized by subtracting appropriate amounts of the lower order terms. The radial variation of Bias, Power, and Primary Spherical are shown in Figure 1.

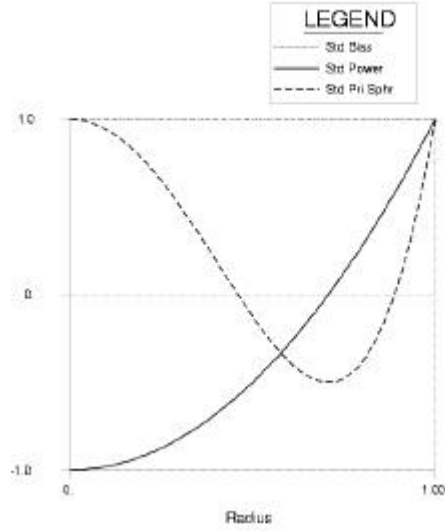


Figure 1. Standard Zernike Bias, Power, Primary Spherical

Products of sine and cosine functions of different order are also orthogonal over a unit circle:

$$\int_0^{2\Pi} \sin(k\Theta) * \sin(m\Theta) d\Theta = \int_0^{2\Pi} \cos(k\Theta) * \cos(m\Theta) d\Theta = 0 \quad \text{for } k \neq m \quad (1.8)$$

making Zernike trefoil orthogonal to Zernike tetrafoil.

1.2 Zernike polynomials

The general form of the Zernike series

$$\Delta Z(\mathbf{r}, \Theta) = A_{00} + \sum_{N=2}^{\infty} A_{N0} R_N^0(\mathbf{r}) + \sum_{N=1}^{\infty} \sum_{M=1}^{\infty} R_N^M [A_{NM} \cos(M\Theta) + B_{NM} \sin(M\Theta)] \quad (1.9)$$

where

$$R_N^M(\mathbf{r}) = \sum_{S=0}^{\frac{N-M}{2}} (-1)^S \frac{(N-S)!}{S! \left(\frac{N+M}{2} - S \right)! \left(\frac{N-M}{2} - S \right)!} \mathbf{r}^{(N-2S)} \quad (1.10)$$

and ρ is the dimensionless normalized radius and Θ is the polar angle. Additional restrictions on the series include that terms only exist when $N-M$ is even and $N \geq M$. The “Standard Zernike” series are given in Born and Wolf¹ and include as many terms as desired. A listing of the Zernike polynomials is provided in the Appendix.

The “Standard Zernike” polynomials as defined above have a value of 1.0 at $\rho=1$. CodeV uses this normalization. The surface RMS of each CodeV unit Zernike polynomial is:

$$\text{Unit axisymmetric polynomial surface RMS} = \left[\sqrt{(N+1)} \right]^{-1}$$

$$\text{Unit non-axisymmetric polynomial surface RMS} = \left[\sqrt{2(N+1)} \right]^{-1}$$

Zemax scales the standard Zernikes so that the RMS of each term has a value 1.0 over the unit circle. The Zemax scale factors are:

$$\text{Axisymmetric terms} = \sqrt{N+1} \tag{1.11}$$

$$\text{Non-axisymmetric terms} = \sqrt{2(N+1)}$$

Thus Zemax Power and Primary Spherical are

$$\tilde{\Phi}_1 = \sqrt{3}(2r^2 - 1) \qquad \tilde{\Phi}_2 = \sqrt{5}(6r^4 - 6r^2 + 1) \tag{1.12}$$

Thus the same finite element surface displacement is represented by different magnitudes in Zemax and CodeV. Unit values of Zemax and CodeV Power and Primary Spherical are shown in Figure 2.

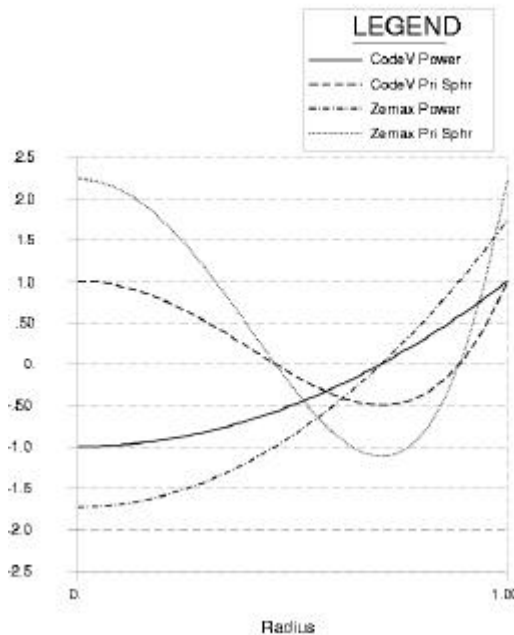


Figure 2. 1 Wave of Power and Primary Spherical

To confuse matters more, CodeV and Zemax place the polynomials in a different order. For instance primary spherical is term 13 in CodeV and term 11 in Zemax. A comparison list of CodeV and Zemax ordering is given in the Appendix.

An alternate set of Zernike terms is called the “Fringe Zernike” set, which is composed of 37 low order terms, including the axisymmetric terms for ρ^{10} and ρ^{12} . The normalization for Fringe Zernikes require that they have a value 1.0 at $\rho=1$, like the Standard Zernikes above. For this particular set, both CodeV and Zemax use the same ordering and normalization. Therefore, Zemax Power for “Standard Zernikes” is scaled to RMS=1, but Zemax Power for “Fringe Zernikes” is not.

1.3 Odd geometries

Zernike orthogonality is lost on any surface other than a full unit circle. Consider the primary mirror of a Cassegrain telescope which includes a central hole of $\rho=0.2$. The orthogonality of Bias and Power (Eqn 7) is now lost:

$$2\Pi \int_{0.2}^1 (1)(2r^2 - 1)rdr = 2\Pi \left[\left(\frac{2}{4} - \frac{1}{2} \right) - \left(\frac{.0032}{4} - \frac{.04}{2} \right) \right] = 0.12 \neq 0 \quad (1.13)$$

As one would expect, orthogonality is also lost on a non-circular geometry, such as a square optic:

$$\int_{-1}^{+1} \int_{-1}^{+1} (1)(2r^2 - 1)dxdy \neq 0 \quad (1.14)$$

2.0 DISCRETE DATA

1.1 Numerical Integration

Finite element analyses provide surface distortions at discrete locations on an optic. For discrete data evaluated at node k , equation (1.1) becomes:

$$\sum_k \Phi_{1k} \Phi_{2k} A_k = 0 \quad (2.1)$$

where A_k is the area associated with node k . Using numerical integration on the Bias(Φ_0), Power(Φ_1), and Primary Spherical(Φ_2) terms, the residual error verses the number of equally spaced radial integration points K over the unit circle is shown in Table 1. The diagonal terms $\Phi_j\Phi_j$ represent the RMS^2 and the off-diagonal terms $\Phi_i\Phi_j$ represent the coupling or non-orthogonality.

Table 1: Numerical integration on a unit circle

K	$\Phi_0\Phi_0$	$\Phi_1\Phi_1$	$\Phi_2\Phi_2$	$\Phi_0\Phi_1$	$\Phi_0\Phi_2$	$\Phi_1\Phi_2$
10	1.0000	.34660	.23838	.00500	.01990	.02460
20	1.0000	.33666	.20990	.00125	.00499	.00623
50	1.0000	.33387	.20160	.00020	.00080	.00100
100	1.0000	.33347	.20040	.00005	.00020	.00025
200	1.0000	.33337	.20010	.00001	.00005	.00006
500	1.0000	.33334	.20002	.00000	.00001	.00001
1000	1.0000	.33333	.20000	.00000	.00000	.00000

Note that the coupling terms drop off as K^2 .

SigFit prints this orthogonality check for surface fitting to any finite element mesh pattern. The data in Table 2 is based on an area weighting calculated internally in SigFit for the finite element areas projected to a flat plane normal to the optical axis. For the polar meshes shown in Figures 3 ($K=10$) and Figure 4 ($K=20$), the Table 2 results correlate closely to Table 1. In fact, the finite element area calculation provides more accurate answers than the area calculation in the Table 1 integration.

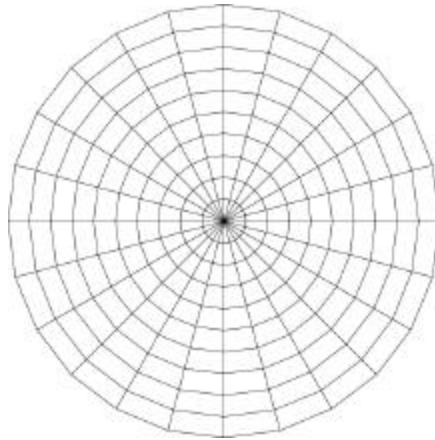


Figure 3. Polar mesh with K=10

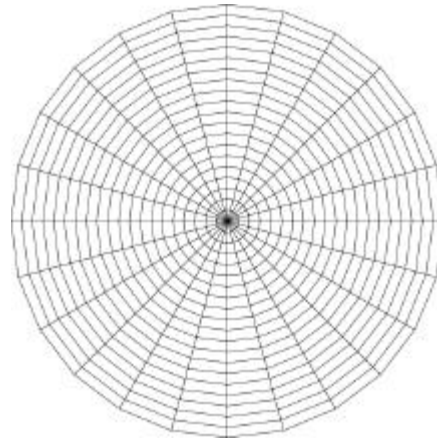


Figure 4. Polar mesh with K=20

Table 2: SigFit integration on polar meshes with projected areas

K	$\Phi_0\Phi_0$	$\Phi_1\Phi_1$	$\Phi_2\Phi_2$	$\Phi_0\Phi_1$	$\Phi_0\Phi_2$	$\Phi_1\Phi_2$
10	1.000	.3462	.2370	.0033	.0193	.0220
20	1.000	.3366	.2095	.0008	.0049	.0056

Table 3 shows the results for area weighting based on the true curved surface area and Table 4 shows the results for all weighting terms set to 1.0.

Table 3: SigFit integration on polar meshes with true curved surface areas

K	$\Phi_0\Phi_0$	$\Phi_1\Phi_1$	$\Phi_2\Phi_2$	$\Phi_0\Phi_1$	$\Phi_0\Phi_2$	$\Phi_1\Phi_2$
10	1.000	.3463	.2374	.0090	.0195	.0246
20	1.000	.3366	.2097	.0066	.0049	.0079

Table 4: SigFit integration on polar meshes with area weighting set to 1.0

K	$\Phi_0\Phi_0$	$\Phi_1\Phi_1$	$\Phi_2\Phi_2$	$\Phi_0\Phi_1$	$\Phi_0\Phi_2$	$\Phi_1\Phi_2$
10	1.000	.4736	.3346	-.2271	.2105	-.1064
20	1.000	.4677	.3191	-.2779	.2105	-.1640

As can be seen from the tables, the projected area provides the best results. Equally weighting nodes (Table 4) which represent different areas provides poor results and should not be used.

1.2 Comparison to dynamic modes

Zernike polynomials are not the only functions which represent orthogonal functions over a unit circle. The dynamic mode shapes for a uniform thickness circular plate are orthogonal with respect to the mass matrix. For any 2 distinct modes i and j ,

$$\Phi_i^T M \Phi_j = 0 \quad (2.2)$$

For discrete data, the above can be written,

$$\sum_k \Phi_{ik} \Phi_{jk} M_k = 0 \tag{2.3}$$

For uniform thickness plates, the mass (M_k) at node k is simply the area (A_k) times thickness and mass density.

The dynamic mode shapes for circular plates² have radial coefficients which are Bessel functions rather than simple polynomials like Zernikes, but the azimuthal terms are identical. The complexity of Bessel functions makes these shapes less desirable.

The dynamic mode shapes were fit with Zernikes in SigFit as shown in Table 5 for the lowest elastic modes. Mode 1 and 2 in Figure 5 are a mode pair which contain only astigmatism terms, of which roughly 95% is primary astigmatism. Mode 3 in Figure 6 contains only axisymmetric terms, of which 90% is power. Other modes contained similar effects. For example, Mode pair 4 & 5 contained only trefoil terms, while mode pair 6 & 7 contained only coma terms, and mode pair 8 & 9 contained only tetrafoil terms. Essentially, the dynamic modes are very similar to the Zernike polynomials except for slight differences in the radial variations.

Table 5. Zernike fit to dynamic modes

```

=====
Sigmadyne, Inc.      SigFit  Version=2002-r1      05-Jun-02  12:33:26
=====
CIRCULAR PLATE - 360 DEG - FREE FREE MODES THIN PLATE
FIRST ELASTIC MODE SHAPE
-----
Order   Aberration      Magnitude   Phase      Residual    Residual
  N M                                (Waves)    (Deg)      RMS          P-V
-----
      Input(wrt zero)
2  2  Pri Astigmatism  1.05943    -12.9      .0200       .1133
4  2  Sec Astigmatism  .06225     77.1       .0015       .0108
6  2  Ter Astigmatism  .00540     -12.9      0.0000      .0001
8  2  Qua Astigmatism  .00005     -12.9      0.0000      .0001
-----

THIRD ELASTIC MODE SHAPE
-----
Order   Aberration      Magnitude   Phase      Residual    Residual
  N M                                (Waves)    (Deg)      RMS          P-V
-----
      Input(wrt zero)
0  0  Bias             .00003     .0         .4978       1.7421
2  0  Power (Defocus) -.85604     .0         .0579       .2085
4  0  Pri Spherical   .12841     .0         .0057       .0300
6  0  Sec Spherical   -.01499     .0         .0002       .0008
8  0  Ter Spherical   .00049     .0         0.0000      .0001
10 0  Qua Spherical   -.00002     .0         0.0000      0.0000
12 0  Qin Spherical   0.00000     .0         0.0000      0.0000

```

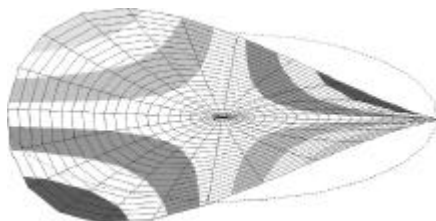


Figure 5. First Elastic Mode Shape

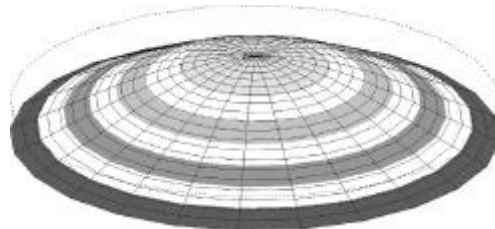


Figure 6. Third Elastic Mode Shape

3.0 ZERNIKE POLYNOMIALS

3.1 Fitting

The mathematics of fitting Zernike polynomials to finite element results is well documented³.

U_k = displacement of grid point k from a finite element solution

$Z_k = \sum_j C_j F_{jk}$ = displacement of grid point k as a sum of Zernike coefficients

F_{jk} = surface displacement of grid k for a unit value of coefficient j

W_k = fraction of area at grid k to the full optic area

Let the error be represented as:

$$E = \sum_k W_k (U_k - Z_k)^2 \quad (3.1)$$

To find the coefficients C_j , minimize the error:

$$dE/dC_j = 0 \quad (3.2)$$

The resulting equations are a linear system, which is easily solved.

$$[H] \{C\} = \{R\} \quad (3.3)$$

where $H_{ji} = \sum_k W_k F_{jk} F_{ik}$ (3.4)

and $R_j = \sum_k W_k U_k F_{jk}$ (3.5)

How well the Zernike coefficients represent the deformed shape is best represented by the residual error after all fitted terms have been removed (see Table 5). In SigFit the residual error is provided as a numerical value for RMS and Peak-Valley and in the form of a nodal file for graphical viewing.

1.2 Coupling

Coupling of Zernikes depends on the form of the optic as well as the finite element mesh.

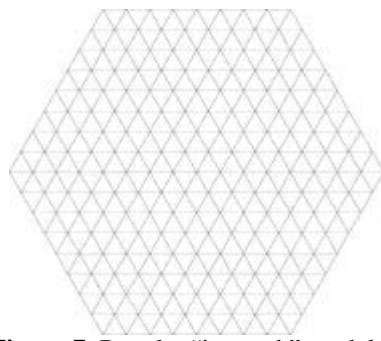


Figure 7. Regular "isomesh" model

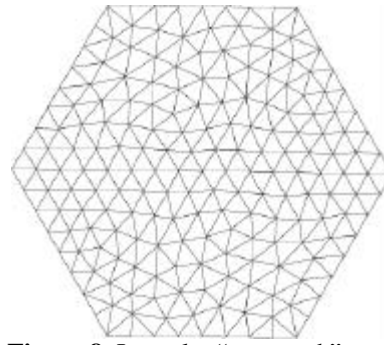


Figure 8. Irregular "automesh" model

The irregular mesh in Figure 8 causes coupling of terms which are not coupled in a regular mesh like Figure 7. In the regular mesh, axisymmetric terms are coupled only to other axisymmetric terms. In the irregular mesh, axisymmetric terms pick up additional coupling with astigmatism, coma, trefoil, etc.

1.3 Fitting Examples

The model in Figure 9 was mounted on 3 points and loaded with 1g along the optical axis. Table 6 shows the Zernike fit results from SigFit. The residual surface RMS after all terms removed was $.05\lambda$ showing that 98% of the surface distortion is represented by the Zernike coefficients. The input and residual surface contour plots in Figure 9 and 10 give a graphical representation of what was not represented by the Zernikes. In this example, we can see that some local distortion around mounts is not well represented, but the amount is small.

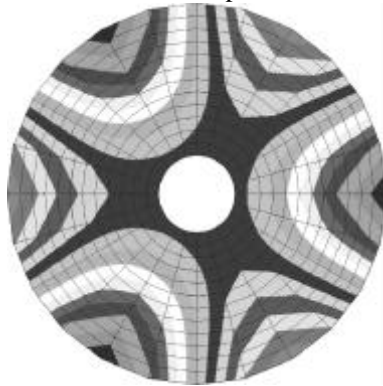


Figure 9. 1g on 3point mount input surface

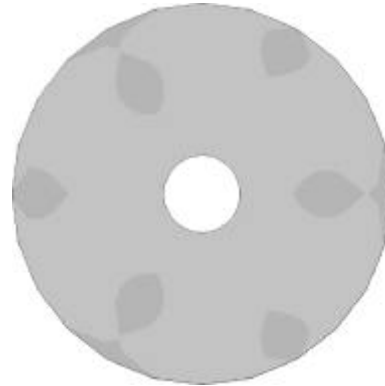


Figure 10. 1g with all Zernikes removed

Table 6: Zernike fit to 1g Z on 3 point mount

Sigmadyne, Inc.		SigFit	Version=2002-r1	23-May-02 09:15:29			

Order	Aberration		Magnitude	Phase	Residual	Residual	
K N M			(Waves)	(Deg)	RMS	P-V	
Input(wrt zero)					2.9302	13.2711	
1	0	0	Bias	-.05862	.0	2.9307	13.2711
2	1	1	Tilt	.00000	.0	2.9307	13.2711
3	2	0	Power (Defocus)	.73829	.0	2.9085	13.2711
4	2	2	Pri Astigmatism	.00000	.0	2.9085	13.2711
5	3	1	Pri Coma	.00000	.0	2.9085	13.2711
6	3	3	Pri Trefoil	7.89198	.0	.5666	2.9184
7	4	0	Pri Spherical	-.59998	.0	.5106	2.5290
8	4	2	Sec Astigmatism	.00000	.0	.5106	2.5290
9	4	4	Pri Tetrafoil	.00000	.0	.5106	2.5290
10	5	1	Sec Coma	.00000	.0	.5106	2.5290
11	5	3	Sec Trefoil	1.56592	60.0	.1905	1.1336
12	5	5	Pri Pentafoil	.00000	.0	.1905	1.1336
13	6	0	Sec Spherical	.13964	.0	.1814	.9335
14	6	2	Ter Astigmatism	.00000	.0	.1814	.9335
15	6	4	Sec Tetrafoil	.00000	.0	.1814	.9335
16	6	6	Pri Hexafoil	.52198	.0	.1206	.8358
17	7	1	Ter Coma	.00000	.0	.1206	.8358
18	7	3	Ter Trefoil	.24919	.0	.0969	.5968
19	7	5	Sec Pentafoil	.00000	.0	.0969	.5968
20	8	0	Ter Spherical	.01856	.0	.0967	.6089
21	8	2	Qua Astigmatism	.00000	.0	.0967	.6089
22	8	4	Ter Tetrafoil	.00000	.0	.0967	.6089
23	8	6	Sec Hexafoil	.29821	30.0	.0536	.2852

The same model was given random set of displacements in Figure 11. As can be seen in the Zernike fit in Table 7, the residual RMS never decreases significantly, even though large values of coefficients are calculated. Basically, the

Zernikes are useless since the shape can not be represented by the low order Zernikes. Figure 12 shows graphically that the residual surface is of the same order as the input surface. To pass this data to an optics code, a finely spaced interferogram array file is required as in Section 4.

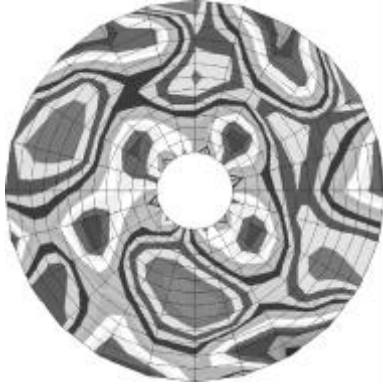


Figure 11. Random Input data -BFP removed

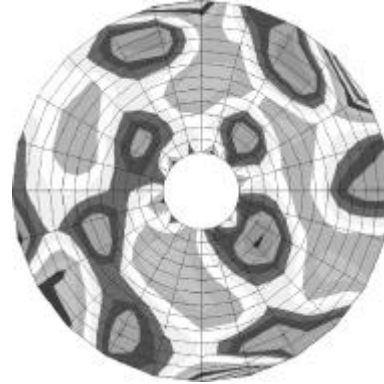


Figure 12 Random - After all Zernikes removed

Table 7. Zernike Fit to Random Data

=====						
Sigmadyne, Inc.		SigFit	Version=2002-r1	11-Jun-02	13:35:26	

Order	Aberration		Magnitude	Phase	Residual	Residual
K	N	M	(Waves)	(Deg)	RMS	P-V
			Input(wrt zero)		3.3806	15.1475
1	0	0	Bias	.0	3.3815	15.1475
2	1	1	Tilt	147.3	3.3815	15.1548
3	2	0	Power (Defocus)	.0	3.3859	15.3773
4	2	2	Pri Astigmatism	78.0	3.3296	15.7127
5	3	1	Pri Coma	-44.5	3.2794	14.7934
6	3	3	Pri Trefoil	30.9	3.2793	14.8031
7	4	0	Pri Spherical	.0	3.0992	14.6889
8	4	2	Sec Astigmatism	-82.4	3.0205	17.2080
9	4	4	Pri Tetrafoil	29.2	2.9517	16.3975
10	5	1	Sec Coma	118.9	2.9473	15.9743
11	5	3	Sec Trefoil	20.9	2.8949	18.2172
12	5	5	Pri Pentafoil	-9.8	2.8536	18.3254

4.0 ALTERNATIVE FORMS

4.1 Other polynomials

Depending on the optical program to be used, other polynomials may be used to fit deformed data. For example in CodeV, both aspheric and X-Y polynomials may be used to describe a surface.

$$Z = \frac{cr^2}{1 + \sqrt{1 - (1+k)c^2 r^2}} + \sum_j A_j r^j \quad (4.1)$$

$$Z = \frac{cr^2}{1 + \sqrt{1 - (1+k)c^2 r^2}} + \sum_j C_j x^M y^N \quad (4.2)$$

Typically, the X-Y polynomials could fit rectangular mirrors which may have rectangular stiffening structure. Whereas, the aspheric polynomials could be used to fit axisymmetric behavior to a very high order. SigFit may optionally fit either of the above polynomial sets.

A variation of the Zernike polynomials exist which are orthogonal over a unit circle containing a hole, as in the Cassegrain primary mirror. Since most optic programs do not allow these as input, they are not discussed here.

4.2 Array interpolation

When FEA data such as pocket quilting in a lightweight mirror is not well described by low order polynomials, an alternate format is available. All optical programs allow array data input since that is the form of interferometric test data. The two surface distortions in Figure 9 and 11 were interpolated in SigFit to provide the array data shown in Figures 13 and 14. When compared to the original surfaces, one can see that the interferogram is an accurate representation of the data. For the smooth data in Figure 9 either representation is good, but for the random data in Figure 11, the array is a much better representation than the Zernike coefficients.

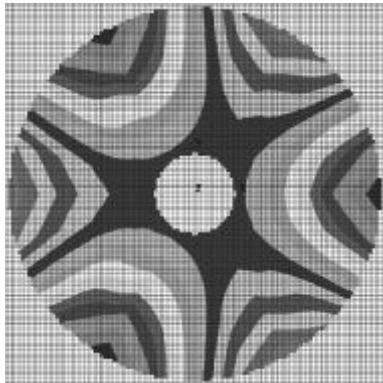


Figure 13. Array for 3 point mount

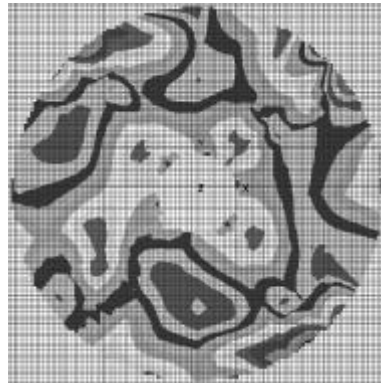


Figure 14. Array for Random data

5.0 SUMMARY

Standard finite element results are usually not in a convenient form for opto-mechanical analysis. The output must be processed in an interface program such as SigFit⁴ to convert it to Zernike polynomials. In the event that the Zernikes do not well represent the data, then interferogram (rectangular array) files must be created. How well the Zernikes fit the data can be determined by comparing the residual RMS to the input RMS, and by plotting the residual surface. For most typical FE models the resulting Zernikes will not be truly orthogonal. The lack of orthogonality does not prevent the Zernikes from being a useful representation of the surface distortion.

6.0 REFERENCES

- 1) M. Born & E. Wolf, *Principles of Optics*, Pergamon Press, New York, 1964.
- 2) R. Blevins, *Formulas for Natural Frequency and Mode Shape*, Krieger Pub., Malabar, FL, 1979
- 3) V. Genberg, "Optical Surface Evaluation", SPIE Proc. Vol. 450, Paper 450-08, Nov 1983.
- 4) SigFit Reference Manual, Sigmadyne, Inc., Rochester, NY, 2002.

7.0 APPENDIX

The following are Zernike numbering and normalization:

N	M	CoV	Zmx	ZFR	Name	Equation	
0	0	Z01	Z01	Z01	Bias	(1)	R=Normalized Radius
1	1	Z02	Z02	Z02	Tilt-X	(R) cos(T)	T=Theta measured from X
1	1	Z03	Z03	Z03	Tilt-Y	(R) sin(T)	N=Radial wave #
2	0	Z05	Z04	Z04	Power	(2R ² -1)	M=Circumferential wave #
2	2	Z04	Z06	Z05	1-Astg-X	(R ²) cos(2T)	CoV=CodeV Std Zernike order
2	2	Z06	Z05	Z06	1-Astg-Y	(R ²) sin(2T)	Zmx=Zemax Std Zernike order
3	1	Z08	Z08	Z07	1-Coma-X	(3R ³ -2R) cos(3T)	ZFR=Fringe Zernike order
3	1	Z09	Z07	Z08	1-Coma-Y	(3R ³ -2R) sin(3T)	
3	3	Z07	Z10	Z10	1-Tref-X	(R ³) cos(3T)	Zemax normalization adds
3	3	Z10	Z09	Z11	1-Tref-Y	(R ³) sin(3T)	coeff =sqrt(N+1) if M=0
4	0	Z13	Z11	Z09	1-Sphr	(6R ⁴ -6R ² +1)	coeff =sqrt(2(N+1)) if M not 0
4	2	Z12	Z12	Z12	2-Astg-X	(4R ⁴ -3R ²) cos(2T)	
4	2	Z14	Z13	Z13	2-Astg-Y	(4R ⁴ -3R ²) sin(2T)	X term=Acos()
4	4	Z11	Z14	Z17	1-Tetr-X	(R ⁴) cos(4T)	Y term=Bsin()
4	4	Z15	Z15	Z18	1-Tetr-Y	(R ⁴) sin(4T)	Magnitude=sqrt(A ² +B ²)
5	1	Z18	Z16	Z14	2-Coma-X	(10R ⁵ -12R ³ +3R) cos(T)	Phase=(1/M)atan(B/A)
5	1	Z19	Z17	Z15	2-Coma-Y	(10R ⁵ -12R ³ +3R) sin(T)	
5	3	Z17	Z18	Z19	2-Tref-X	(5R ⁵ -4R ³) cos(3T)	
5	3	Z20	Z19	Z20	2-Tref-Y	(5R ⁵ -4R ³) sin(3T)	
5	5	Z16	Z20	Z26	1-Pent-X	(R ⁵) cos(5T)	
5	5	Z21	Z21	Z27	1-Pent-Y	(R ⁵) sin(5T)	
6	0	Z25	Z22	Z16	2-Sphr	(20R ⁶ -30R ⁴ +12R ² -1)	
6	2	Z24	Z24	Z21	3-Astg-X	(15R ⁶ -20R ⁴ +6R ²) cos(2T)	
6	2	Z26	Z23	Z22	3-Astg-Y	(15R ⁶ -20R ⁴ +6R ²) sin(2T)	
6	4	Z23	Z26	Z28	2-Tetr-X	(6R ⁶ -5R ⁴) cos(4T)	
6	4	Z27	Z25	Z29	2-Tetr-Y	(6R ⁶ -5R ⁴) sin(4T)	
6	6	Z22	Z28		1-Hexa-X	(R ⁶) cos(6T)	
6	6	Z28	Z27		1-Hexa-Y	(R ⁶) sin(6T)	
7	1	Z32	Z30	Z23	3-Coma-X	(35R ⁷ -60R ⁵ +30R ³ -4R) cos(T)	
7	1	Z33	Z29	Z24	3-Coma-Y	(35R ⁷ -60R ⁵ +30R ³ -4R) sin(T)	
7	3	Z31	Z32	Z30	3-Tref-X	(21R ⁷ -30R ⁵ +10R ³) cos(3T)	
7	3	Z34	Z31	Z31	3-Tref-Y	(21R ⁷ -30R ⁵ +10R ³) sin(3T)	
7	5	Z30	Z34		2-Pent-X	(7R ⁷ -6R ⁵) cos(5T)	
7	5	Z35	Z33		2-Pent-Y	(7R ⁷ -6R ⁵) sin(5T)	
7	7	Z29	Z36		1-Sept-X	(R ⁷) cos(7T)	
7	7	Z36	Z35		1-Sept-Y	(R ⁷) sin(7T)	
8	0	Z41	Z37	Z25	3-Sphr	(70R ⁸ -140R ⁶ +90R ⁴ -20R ² +1)	
8	2	Z40	Z38	Z32	4-Astg-X	(56R ⁸ -105R ⁶ +60R ⁴ -10R ²) cos(2T)	
8	2	Z42	Z39	Z33	4-Astg-Y	(56R ⁸ -105R ⁶ +60R ⁴ -10R ²) sin(2T)	
8	4	Z39	Z40		3-Tetr-X	(28R ⁸ -42R ⁶ +15R ⁴) cos(4T)	
8	4	Z43	Z41		3-Tetr-Y	(28R ⁸ -42R ⁶ +15R ⁴) sin(4T)	
8	6	Z38	Z42		2-Hexa-X	(8R ⁸ -7R ⁶) cos(6T)	
8	6	Z44	Z43		2-Hexa-Y	(8R ⁸ -7R ⁶) sin(6T)	
8	8	Z37	Z44		1-Octa-X	(R ⁸) cos(8T)	
8	8	Z45	Z45		1-Octa-Y	(R ⁸) sin(8T)	
9	1	Z50	Z46	Z34	4-Coma-X	(126R ⁹ -280R ⁷ +210R ⁵ -60R ³ +5R) cos(T)	
9	1	Z51	Z47	Z35	4-Coma-Y	(126R ⁹ -280R ⁷ +210R ⁵ -60R ³ +5R) sin(T)	
10	0	Z61	Z56	Z36	4-Sphr	(252R ¹⁰ -630R ⁸ +560R ⁶ -210R ⁴ +30R ² -1)	
12	0	Z73	Z79	Z37	5-Sphr	(924R ¹² -2772R ¹⁰ +3150R ⁸ -1680R ⁶ +420R ⁴ -42R ² +1)	